

Corrugated Sectorial Leaky-Wave Antenna for DoA applications

*Original*

Corrugated Sectorial Leaky-Wave Antenna for DoA applications / Perrone, Matteo; Sarrazin, Julien; Valerio, Guido; Lombardi, Guido. - ELETTRONICO. - (2025). ( 25th International Symposium on Electromagnetic Theory (EMTS 2025) Bologna (Ita) 23-27 June 2025) [10.46620/URSIEMTS25/GANP7276].

*Availability:*

This version is available at: 11583/3001540 since: 2026-01-15T12:48:29Z

*Publisher:*

IEEE

*Published*

DOI:10.46620/URSIEMTS25/GANP7276

*Terms of use:*

This article is made available under terms and conditions as specified in the corresponding bibliographic description in the repository

*Publisher copyright*

IEEE postprint/Author's Accepted Manuscript

©2025 IEEE. Personal use of this material is permitted. Permission from IEEE must be obtained for all other uses, in any current or future media, including reprinting/republishing this material for advertising or promotional purposes, creating new collecting works, for resale or lists, or reuse of any copyrighted component of this work in other works.

(Article begins on next page)

## Corrugated Sectorial Leaky-Wave Antenna for DoA applications

Matteo Perrone<sup>\*(1)</sup>, Julien Sarrazin<sup>(2)</sup>, Guido Valerio<sup>(2)</sup>, Guido Lombardi<sup>(1)</sup>

(1) Department of Electronics and Telecommunications (DET), Politecnico di Torino, 10129, Turin, Italy  
{matteo\_perrone, guido.lombardi}@polito.it

(2) Sorbonne Université, CNRS, Laboratoire de Génie Electrique et Electronique de Paris, 75252, Paris, France  
Université Paris-Saclay, CentraleSupélec, CNRS, Laboratoire de Génie Electrique et Electronique de Paris, 91192,  
Gif-sur-Yvette, France.  
{julien.sarrazin, guido.valerio}@sorbonne-universite.fr

### Abstract

The beam-scanning capability with frequency of leaky-wave antennas facilitates Direction-of-Arrival (DoA) estimation by offering less complex solutions than array-based methods. In this work, a corrugated sectorial LWA is analyzed for DoA application. In particular, an analytical model and the Adjacent-Zeros Method (AZM) are used to increase the dispersion of the antenna and thus reduce the required frequency to achieve the desired beam-scanning. Using the Multiple Signal Classification (MUSIC) algorithm the correct DoA estimation is demonstrated, and the origin of ambiguities due to the symmetry of the antenna is discussed.

### 1 Introduction

Metasurfaces, as an emerging class of engineered materials, have shown significant potential in revolutionizing antenna design, particularly in the context of millimeter-wave (mm-wave) communications and sensing applications. They are low-cost and passive structures that can provide a solution to modify the phase and amplitude distribution of surface and guided waves. They also introduce or modify the frequency dispersion of an electromagnetic device, without recurring to inhomogeneous materials or active components. As an example, the introduction of periodic corrugations along the lower plate of a waveguide and periodic slots along its upper plate results in a controlled leakage of energy, allowing the beam-scanning properties of the antenna to vary with frequency [1], [2]. This frequency-dependent scanning ability offers significant advantages over traditional mechanically steered antennas by providing continuous beam steering or electronic control. This flexibility makes these systems suitable for applications such as Direction-of-Arrival (DoA) estimation in complex environments. In this context, the Multiple Signal Classification (MUSIC) algorithm, a widely-used high-resolution technique, proved effective for DoA estimation. By exploiting the spatial covariance matrix of received signals, MUSIC provides an efficient method for signal resolution in high angular resolution environments. This paper explores the

synergy between metasurfaces, radiating guided structures, and signal-processing techniques to address the growing demand for low-cost and passive sensing units to be employed in smart surfaces in mmWave communications. We aim to demonstrate that such systems, capable of real-time frequency-beam-scanning, can enable next-generation sensing and communication technologies, offering promising solutions for a wide range of applications, from wireless networks to radar and beyond. This paper is organized as follows. Section 2 describes the geometry of the corrugated sectorial waveguide and the dispersion diagram is obtained with Adjacent-Zeros Method (AZM). In Section 3 a LWA is designed by etching circular slots on the upper plate and the simulated results are presented. Section 4 performs DoA estimation using the proposed LWA through MUSIC algorithm. In Section 5, conclusions are drawn.

### 2 Corrugated sectorial waveguide

We study a new sectorial leaky-wave antenna starting from the work in [1]. In particular, a corrugated sectorial waveguide with circular slots is analyzed (Fig. 1). In a cylindrical coordinate system  $(\rho, \phi, z)$ , the waveguide has a wedge-shaped geometry with lateral plates at  $\phi = 0, \phi_0$  and horizontal plates at  $z = 0, b$ , where  $\phi_0$  is the aperture angle. In this structure, a single  $TM^z$  mode propagates [1]. Following the procedure proposed in [1], we build concentric circular corrugations on the lower plate of the sectorial waveguide. The geometry of the corrugated sectorial waveguide without slots is shown in Fig. 1(a). The period and the width of the corrugations are  $p_c = 2$  mm and  $w_c = 1$  mm, respectively. Each corrugation can be treated as a short-circuited transmission line [3]. The objective is to maximize the dispersion of the waveguide, i.e. to decrease the slope of the dispersion curve in a Brillouin diagram  $f$  vs.  $\beta$ , where  $f$  and  $\beta$  are the frequency and the radial phase constant of the wave propagating in the structure. Corrugations can increase the frequency dispersion of the structure if the working frequency range is close to a band gap. In our case, for mm-wave sensing applications, the chosen range is [26.5, 29.5] GHz. By varying the height of the corrugations  $h_c$ , we evaluated the band gap with the analyti-

cal model in [4] for a parallel-plate waveguide with straight corrugations. We used that model for soft polarization, i.e. for a wave propagation direction perpendicular to the corrugations. Using Ansys HFSS software and the Adjacent Zeros Method (AZM) of [1], we choose  $h_c = 6.5$  mm. The dispersion diagram obtained is shown in Fig. 2.

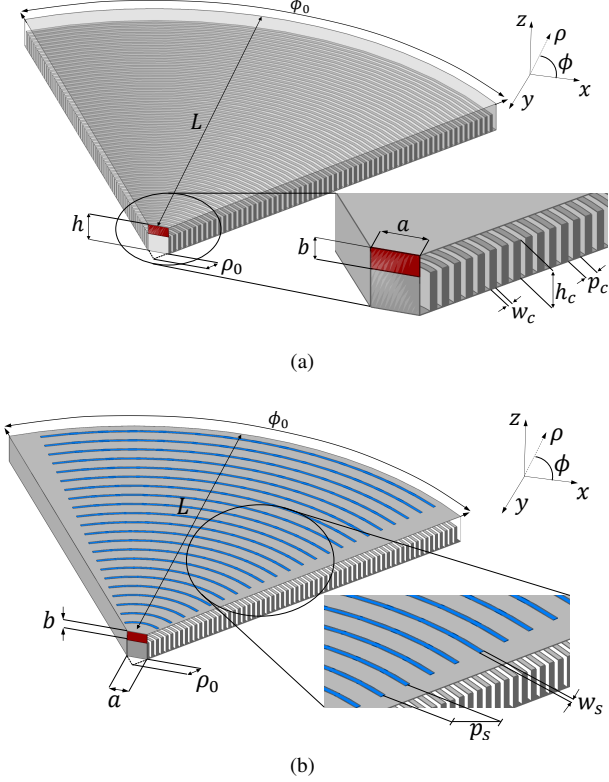


**Figure 1.** Sectorial waveguides studied in this paper. (a) Closed sectorial waveguide with corrugated lower plate. (b) Open sectorial waveguide with circular slots and corrugated lower plate. The geometric parameters are  $\phi_0 = 73^\circ$ ,  $L = 131.5$  mm,  $\rho_0 = 4.8$  mm,  $a = 7.112$  mm,  $b = 3.556$  mm,  $h_c = 6.5$  mm,  $p_c = 2$  mm,  $w_c = 1$  mm,  $p_s = 5.8$  mm,  $w_s = 1.08$  mm.

### 3 Periodic leaky-wave antenna

As shown in Fig. 2,  $\beta$  values are in the slow-range, i.e.  $\beta > k_0$ , while  $\beta$  must be in the fast-range in order to radiate [5]. Periodic modulations can lead to radiation producing infinite higher harmonics, some of which may be in the fast-range and radiate. The approach chosen here is to etch a series of concentric circular slots with the same width and with the same radial distance between them on the upper plate. This structure is not periodic (i.e. invariant under translation) but homothetic (i.e. invariant under radial scaling). However, it is possible to define a linearized periodic structure consisting of a corrugation in Cartesian coordinates orthogonal to the radial direction, which describes well the radiation features of the sectorial waveguide. Its period  $p_s$  must be chosen according to the formula for the higher space harmonics  $\beta_n$  and beam direction  $\theta_n$  in the  $(\rho - z)$  plane [5]:

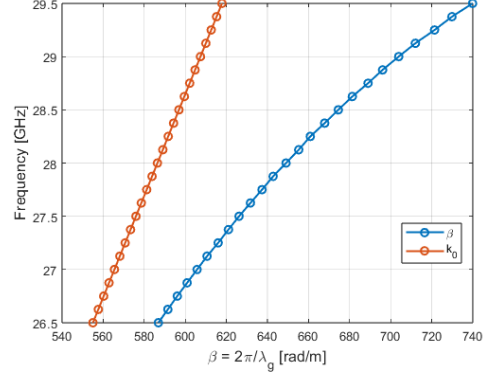


**Figure 2.** Dispersion diagram (frequency vs.  $\beta$ , where  $\beta$  is the radial phase constant of the wave propagating in the waveguide) for the closed corrugated sectorial waveguide of Fig. 1(a) with  $h_c = 6.5$  mm.  $k_0$  is the line of the light.

$$\beta_n = \beta + \frac{2n\pi}{p_s}, \quad n = 0, \pm 1, \pm 2, \dots \quad (1a)$$

$$\theta_n = \sin^{-1}(\beta_n/k_0), \quad (1b)$$

where  $\beta$  is the phase constant of the fundamental mode. As in [1], we build circular and concentric equispaced slots on the upper plate of the sectorial waveguide, producing a periodic leaky-wave antenna. Varying  $p_s$ , fast space harmonics can be generated. We chose  $p_s = 5.8$  mm in order to have a single backward beam as shown in the dispersion diagram of Fig. 3.

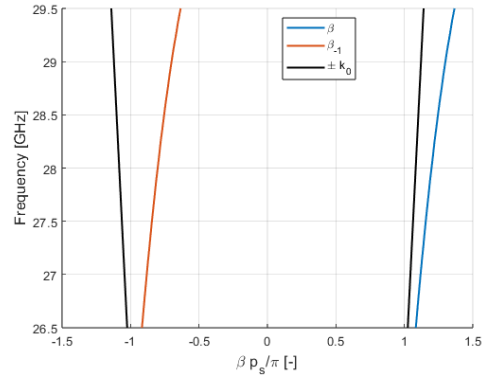


**Figure 3.** Dispersion diagram for the periodic 2D leaky-wave antenna of Fig. 1(b). A single backward beam,  $\beta_{-1}$ , is present.  $\beta$  and  $\pm k_0$  represent the phase constant of the fundamental mode and the lines of light, respectively.

The slot width is  $w_s = \lambda_0/10 = 1.08$  mm, where  $\lambda_0$  is the wavelength in free-space at central frequency 28 GHz, and 22 slots are etched on the upper plate. The geometry of the periodic leaky-wave antenna is illustrated in Fig. 1(b). The coefficient  $|S_{11}|$  is shown in Fig. 4. In the whole frequency band the antenna is well matched with values lower than  $-10$  dB. The realized gain as a function of  $\theta$  angles is shown in Fig. 5. The frequency-beam-scanning

is noticeable for the  $-1$  space harmonics in the  $\theta$  range  $[-67^\circ, -35^\circ]$  as expected using the formula (1b).

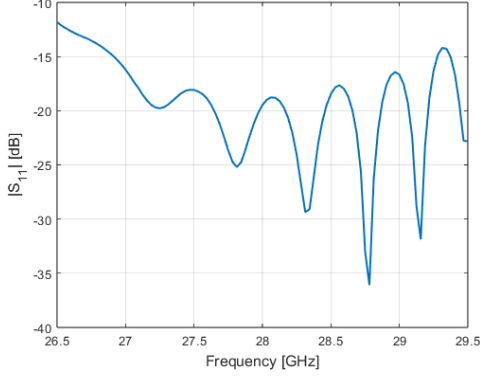


**Figure 4.** Simulated reflection coefficient of the corrugated leaky-wave antenna of Fig. 1(b).

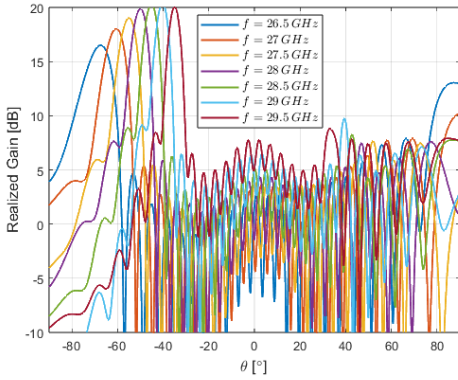


**Figure 5.** Realized gain of the corrugated leaky-wave antenna.

In Fig. 6, the 2D realized gain for three different frequencies is shown. The frequency-beam-scanning for the backward beam is observable. In addition, in the plane swept by  $\phi$  angle, the corrugated leaky-wave antenna has a field of view for  $53.5^\circ < \phi < 126.5^\circ$ , for this reason we do not observe radiation out of this  $\phi$  range. If we observe the 2D realized gain at 28 GHz, the maximum at this frequency is  $\theta = -50^\circ$ . Keeping these two values of frequency and  $\theta$  fixed and taking different  $\phi$ , the value of  $\theta$  does not vary. This can be extended to the other frequencies. This means that the antenna is isotropic along  $\phi$ .

## 4 Direction-of-Arrival estimation

### 4.1 MUSIC applied to LWA

The MUSIC algorithm is a method that allows to estimate the DoA of incoming signals by analyzing the covariance matrix of signals received by an antenna array or LWA in our work. It identifies the directions (or angles) where signal sources are located based on the properties of the received signal and noise, providing high-resolution estimates of DoA. The MUSIC algorithm is employed to esti-

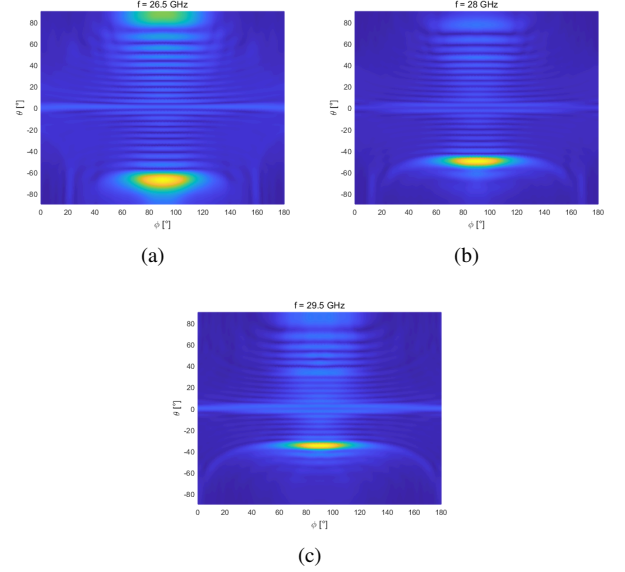


**Figure 6.** Realized gain in the  $\phi - \theta$  plane for three frequencies.

mate the direction of arrival (DoA) of  $D$  sources impinging on the LWA. The system model assumes that the  $D$  sources use a multicarrier modulation scheme, where all subcarriers convey the same data. In general, the signal received by the LWA can be expressed in the frequency domain as:

$$\mathbf{x}[k] = \mathbf{A}(\theta_d, \phi_d) \mathbf{s}[k] + \mathbf{z}[k], \quad (2)$$

where  $\mathbf{x} \in \mathbb{C}^{M \times 1}$  is the received vector,  $M$  is the number of frequency samples,  $k = 1, \dots, K$  is the  $k$ th snapshot among  $K$ ,  $\mathbf{A} \in \mathbb{C}^{M \times D}$  is the LWA response matrix,  $\mathbf{s} \in \mathbb{C}^{D \times 1}$  is the source vector, representing the complex amplitudes of the  $D$  sources and  $\mathbf{z} \in \mathbb{C}^{M \times 1}$  is a complex Additive White Gaussian Noise (AWGN) vector with uncorrelated components. Each column of  $\mathbf{A}$  corresponds to the frequency response of the LWA for a specific incident plane wave with DoA  $(\theta_d, \phi_d)$ ,  $d = 1, \dots, D$  and is obtained through HFSS simulations. It is important to note that  $M$  here represents the number of frequency samples, i.e. subcarriers, as opposed to the number of array elements in a traditional linear-array-based MUSIC scenario. To estimate the DoA, the covariance matrix is first computed from the received signal as:

$$\hat{\mathbf{R}} = \frac{1}{K} \sum_{k=1}^K \mathbf{x}[k] \mathbf{x}^H[k], \quad (3)$$

where  $(\cdot)^H$  denotes the Hermitian transpose. In practice, the covariance matrix is estimated using a finite number of snapshots. The null space of the covariance matrix is computed, and the MUSIC pseudo-spectrum is defined as:

$$P(\theta, \phi) = \frac{1}{\mathbf{a}^H(\theta, \phi) \mathbf{E}_N \mathbf{E}_N^H \mathbf{a}(\theta, \phi)}, \quad (4)$$

where:  $\mathbf{a}(\theta, \phi)$  is the steering vector for an incoming wave at angles  $(\theta, \phi)$ ,  $\mathbf{E}_N$  is the noise subspace of the covariance matrix  $\hat{\mathbf{R}}$ . Peaks in the pseudo-spectrum correspond to the estimated DoAs of the incoming signals.

## 4.2 Results and ambiguities

Simulated MUSIC pseudospectrum is shown in Fig. 7. The simulation is performed with  $D = 1$  incoming source DoA  $\theta_1 = -40^\circ$ ,  $\phi_1 = 77^\circ$ . These values are in the field of view of the the LWA in the frequency bandwidth of the signal. In the simulation, a Signal-to-Noise Ratio (SNR) of 10 dB,  $K = 100$  snapshots and  $M = 49$  frequency samples are selected. In Fig. 7 the true DoA is indicated with red circle, while black point indicate the detection of the MUSIC algorithm. For Fig. 7 the red circle and the black point match and this means that there is a correct detection of DoA. A second peak is visible in the MUSIC pseudospectrum and it reveals an ambiguity in the DoA estimation. This is related to the symmetry of the antenna with respect to the  $yz$  plane ( $\phi = 90^\circ$ ), and consequently to the presence of an image peak for every  $\phi$  between  $0^\circ$  and  $90^\circ$  within the field of view of the antenna.

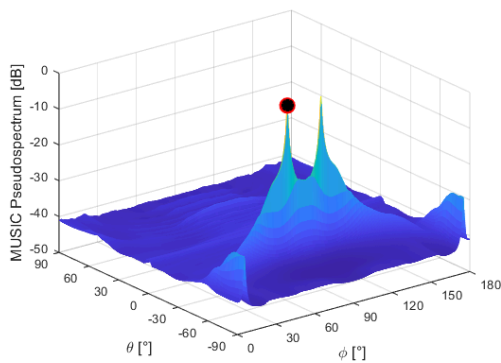


**Figure 7.** 2D MUSIC pseudospectrums obtained with  $D = 1$  DoA  $(\theta, \phi) = (-40^\circ, 77^\circ)$ ,  $SNR = 10$  dB,  $K = 100$  snapshots and  $M = 49$  frequency samples.

## 5 Conclusions

A corrugated periodic leaky-wave antenna have been studied. In particular, using an analytical model and the Adjacent Zeros Method it was possible to choose the height of the corrugations  $h_c$  in order to maximize the dispersion of the antenna. In addition, using MUSIC algorithm, the DoA was correctly estimated, except the possible presence of an ambiguity in  $\phi$  due to the mirror-symmetric geometry of the antenna. To eliminate this ambiguity, a new shape of the corrugations will be implemented to break the symmetry of the structure and of its radiation pattern.

## 6 Acknowledgements

This work was supported by the ANR BeSensiCom project, grant ANR22-CE25-0002 of the French Agence Nationale de la Recherche, Italian PRIN Grant 2017NT5W7Z GREEN TAGS, and Next Generation EU within PNRR M4C2, Inv. 1.4-Avv. n.3138 6/12/2021-CN00000013 National Centre for HPC, Big Data and Quantum Computing.

## References

- [1] M. Perrone, J. Sarrazin, G. Valerio, G. Lombardi, “Leaky-wave analysis and design of a corrugated sectoral waveguide,” *International Conference on Electromagnetics in Advanced Applications (ICEAA)*, pp. 662–666, Sept. 2024, Lisbon, Portugal, doi:10.1109/ICEAA61917.2024.10701709.
- [2] J. Sarrazin, G. Valerio, “H-plane-scanning multi-beam leaky-wave antenna for wide-angular-range AoA estimation at mm-wave”, *17th European Conference on Antennas and Propagation (EuCAP)*, pp. 1-4, Mar. 2023, Florence, Italy, doi: 10.23919/EuCAP57121.2023.10133492.
- [3] C. Balanis, “Rectangular cross-section waveguides and cavities” in *Advanced engineering electromagnetics*, 2nd ed., Wiley, 2012, ch. 8.
- [4] M. Bosiljevac, Z. Sipus, P.-S. Kildal “Construction of Green’s functions of parallel plates with periodic texture with application to gap waveguides—a plane-wave spectraldomain approach,” *IET Microw. Antennas Propag.*, **4**, 11, 2010, pp. 1799–1810, doi:10.1049/iet-map.2009.0399.
- [5] A. A. Oliner, “Leaky-wave antennas” in *Antenna Engineering Handbook*, J. L. Volakis, 4th ed., McGraw-Hill Education, 2007, ch. 11.